Radiation Physics and Chemistry 81 (2012) 410–413

Contents lists available at SciVerse ScienceDirect

Radiation Physics and Chemistry

journal homepage: www.elsevier.com/locate/radphyschem

MeV Si ions bombardments effects on thermoelectric properties of SiO_2/SiO_2+Ge nanolayers

S. Budak [a,*], C. Smith [b], M. Pugh [c], K. Heidary [a], T. Colon [d], R.B. Johnson [c], C. Muntele [b], D. ila [e]

[a] Department of Electrical Engineering and Computer Science, Alabama A&M University, Normal, AL, USA
[b] Center for Irradiation of Materials, Alabama A&M University, Normal, AL, USA
[c] Department of Physics, Alabama A&M University, Normal, AL, USA
[d] Department of Mechanical Engineering, Alabama A&M University, Normal, AL, USA
[e] Department of Physics, Fayetteville St. University, Fayetteville, NC, USA

ARTICLE INFO

Article history:
Received 18 February 2011
Accepted 23 December 2011
Available online 29 December 2011

Keywords:
Ion bombardment
Thermoelectric properties
Multi-nanolayers
Figure of merit

ABSTRACT

The performance of the thermoelectric materials and devices is shown by a dimensionless figure of merit, $ZT=S^2\sigma T/K$, where S is the Seebeck coefficient, σ is the electrical conductivity, T is the absolute temperature and K is the thermal conductivity. ZT can be increased by increasing S, increasing σ, or decreasing K. We have prepared the thermoelectric generator device of SiO_2/SiO_2+Ge multilayer superlattice films using the ion beam assisted deposition (IBAD). The 5 MeV Si ion bombardments have been performed using the AAMU Pelletron ion beam accelerator at five different fluences to make quantum structures (nanodots and/or nanoclusters) in the multilayer superlattice thin films to decrease the cross plane thermal conductivity, increase the cross plane Seebeck coefficient and cross plane electrical conductivity. To characterize the thermoelectric generator devices before and after MeV Si ions bombardments at the different fluences we have measured the cross-plane Seebeck coefficient, the cross-plane electrical conductivity, and the cross-plane thermal conductivity, Raman spectra to get some information about the sample structure and bond structures among the used elements in the superlattice thin film systems.

1. Introduction

The growing concern over increasing energy cost and global warming associated with fossil fuel sources has stimulated the search for cleaner, more sustainable energy sources (Xiao et al., 2008). Thermoelectric devices are solid state devices. They are reliable energy converters and have no noise or vibration as there are no mechanical moving parts (Riffat and Ma 2003). Most applications of thermoelectricity deal with cooling and power generation, both based on thermal and electrical conversion (Bourgault et al., 2008; Budak et al., 2007; Budak et al., 2009). The theory of thermoelectric power generation and thermoelectric refrigeration was first presented by Altenkirch in 1990 (Xi et al., 2007). In thermoelectric generators, the Seebeck effect is used for the direct conversion of a temperature difference into an electric potential between a material pair junction, the thermocouple (Huesgen et al., 2008). Thermoelectric energy conversion is a field that can greatly benefit from the nanoscale heat transport phenomenon (Goldsmid 1964). The efficiency of the thermoelectric devices is limited by the material properties of n-type and p-type semiconductors (Brian 2002). The best thermoelectric materials were succinctly summarized as "phonon-glass electron-crystal", which means that the materials should have a low lattice thermal conductivity as in glass, and high electrical conductivity as in crystals (Slack 1995). The efficiency of the thermoelectric devices is determined by the figure of merit ZT (Guner et al., 2008). The figure of merit is defined by $ZT=S^2\sigma T/\kappa$, where S is the Seebeck coefficient, σ is the electrical conductivity, T is the absolute temperature, and κ is the thermal conductivity (Huang et al., 2005). ZT can be increased by increasing S, by increasing σ, or by decreasing κ. In order to compete with conventional refrigerators, a ZT of 3 is required. Due to their limited energy conversion efficiencies (i.e. ZT is $\sim$1); thermoelectric devices currently have a rather narrow set of applications. However, there is a reinvigorated interest in the field of thermoelectrics due to classical and quantum mechanical size effects, which provide additional ways to enhance energy conversion efficiencies in nanostructured materials (Xiao et al., 2008). It has been shown that the figure of merit can be improved by reducing the lattice thermal conductivity contributing about 75% of the total thermal conductivity. Phonon-grain boundary scattering has a significant effect in reducing the lattice thermal conductivity of

* Corresponding author. Tel.: +1 256 372 5894; fax: +1 256 372 5855.
E-mail address: satilmis.budak@aamu.edu (S. Budak).

0969-806X/$ - see front matter © 2011 Elsevier Ltd. All rights reserved.
doi:10.1016/j.radphyschem.2011.12.035

semiconductor alloys when the phonon mean free path or wavelength is comparable to the grains dimensions without affecting Seebeck coefficient and electrical conductivity (Dughaish 2002). Understanding the thermal conductivity and heat transfer processes in thin films and superlattice structures is critical for the development of microelectronic and optoelectronic devices and low-dimensional thermoelectric and thermionic devices. Experimental results on the thermal conductivity of superlattices have been reported in recent years for several material systems, including GaAs/AlAs, GaAs/AlGaAs, Si/SiGe, Si/Ge and Bi_2Te_3/Sb_2Te_3. These studies demonstrated that the thermal conductivity of a superlattice could be much lower than that estimated from the bulk values of its constituent materials, and even smaller than the thermal conductivity values of the equivalent composition alloys (Borca-Tasiuc et al., 2000). In this study we report on the growth of SiO_2/SiO_2+Ge multilayer superlattice thin film systems using the ion beam assisted deposition (IBAD), and high energy Si ions bombardment of the films for reducing thermal conductivity and increasing electrical conductivity due to the nanoclusters effect during the MeV Si ion bombardments and Raman spectra at different fluences of MeV Si ions bombardment to get some information about the sample structure and bond structures among the used elements in the superlattice thin film systems.

2. Experimental

We have deposited the 50 alternating layers of SiO_2/SiO_2+Ge nanolayers thin films on silicon and silica (suprasil) substrates with the ion beam assisted deposition (IBAD). The multilayer films were sequentially deposited to have a periodic structure consisting of alternating SiO_2 and SiO_2+Ge layers. These thin films constitute a periodic quantum well structure consisting of 50 alternating layers of total thickness of 117 nm. The two electron-gun evaporators for evaporating the two solids were turned on and off alternately to make multilayers. The base pressure obtained in IBAD chamber was about 5×10^{-6} Torr during the deposition process. The growth rate was monitored by a gold coated INFICON Quartz Crystal Monitor (QCM). The film geometries used for deposition of SiO_2/SiO_2+Ge nanolayers thin films are shown in Figs. 1a and b for the thermal conductivity and for Seebeck coefficient measurements respectively.

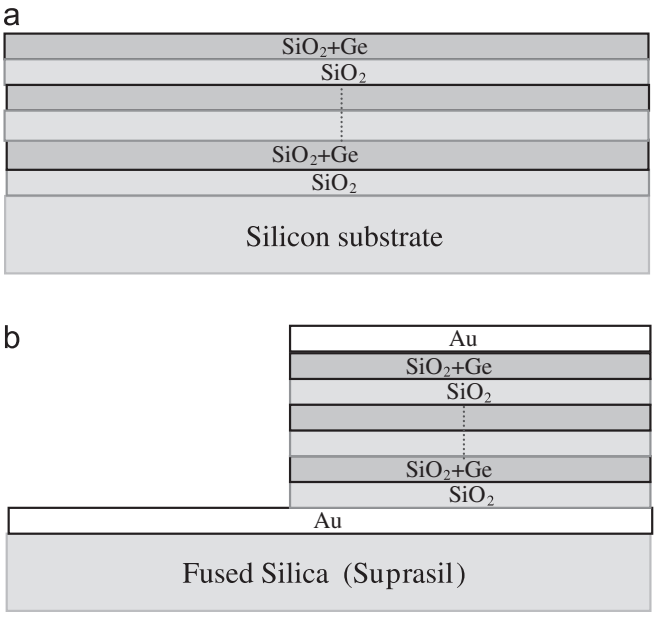

Fig. 1. Geometry of sample from the cross-section, (a) for thermal conductivity, (b) for Seebeck measurements.

The electrical conductivity was measured by the four probe contact system and the thermal conductivity was measured by the 3ω (3rd harmonic) technique. The electrical conductivity, thermal conductivity and Seebeck coefficient measurements have been performed at room temperature. Detailed information about the 3ω (3rd harmonic) technique may be found in Refs. Holland and Smith (1966; Cahill et al., 1994; Tasciuc et al., 2001). In order to make nano structures (nano dots and/or nano clusters) in the layers, 5 MeV Si ions bombardments were performed with the Pelletron ion beam accelerator at the Alabama A&M University Center for Irradiation of Materials (AAMU-CIM). The energy of the bombarding Si ions was chosen by the SRIM simulation software. The five different fluences used for the bombardment were between 1×10^{12} ions/cm^2 and 7×10^{13} ions/cm^2. Dilor-JOBIN YVON-SPEX Raman Spectrometer was used to analyze the multilayer films for order of the system and the bonds among the introduced elements in the multilayer systems.

3. Results and discussion

Fig. 2 shows the Seebeck coefficient temperature dependence of SiO_2/SiO_2+Ge multilayer thin films at different fluences. As seen from Fig. 2, the MeV Si ions bombardments showed positive effects on the Seebeck coefficient at the suitable fluences. Seebeck coefficient measurements showed the n-type behavior for our sample since the sample has the charge carriers of electrons. Seebeck coefficient of the sample depending on the temperature at the different fluences showed an increment in the negative axis direction. As seen from Fig. 2, the maximum effect in Seebeck coefficient could be seen the room temperature for the current multilayer film systems bombarded at the fluence of 5×10^{12} ions/cm^2. If one could look at the Fig. 2, it can be seen that the maximum effect occurred at the fluence of 5×10^{12} ions/cm^2 for this multi-layer film system while the temperature is being increased from 300 K to 380 K. The second positive effective results on the Seebeck coefficient could be seen at the fluence of 7×10^{13} ions/cm^2.

Fig. 3 shows the Raman analysis of SiO_2/SiO_2+Ge amorphous multilayer films at different fluences. Dilor-JOBIN YVON-SPEX Raman Spectrometer was used to analyze the multilayer films for order of the system and the bonds among the introduced elements in the multilayer systems. The Raman spectra of amorphous SiGe consist of three broad bands corresponding to the modes of Ge ± Ge, Si ± Ge and Si ± Si bonds respectively (Gole and Dixon 1998; Klein et al., 1974). We have defined peaks suggesting a Ge-Ge contribution at the polycrystalline layers at 200 cm^{-1}. We have a sharp high intensity peak suggesting a

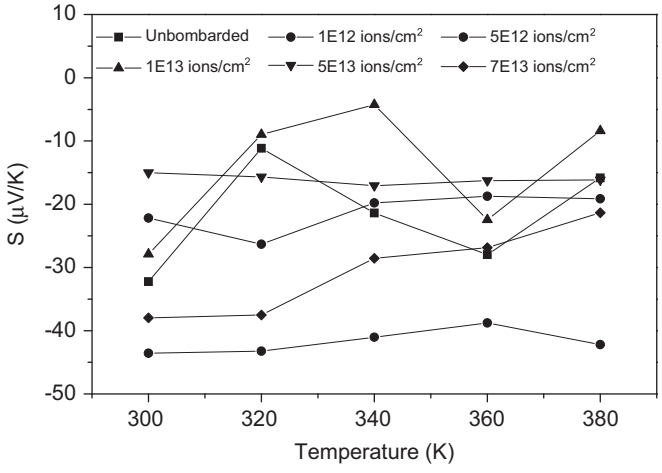

Fig. 2. Seebeck coefficient temperature dependence of SiO_2/SiO_2+Ge multilayer thin films at different fluences.

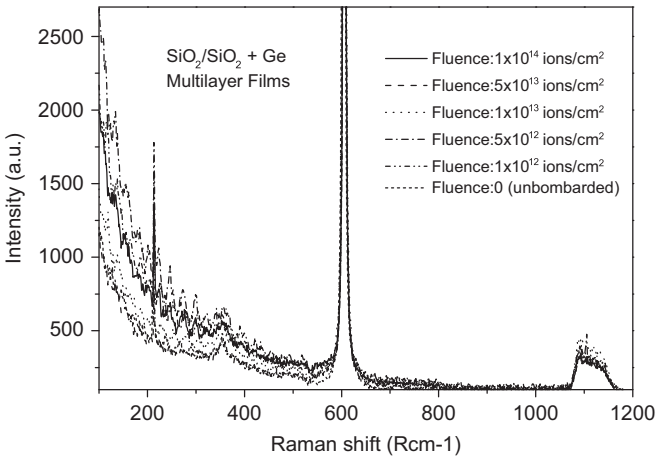

Fig. 3. Raman analysis of SiO_2/SiO_2+Ge multilayer thin films at different fluences.

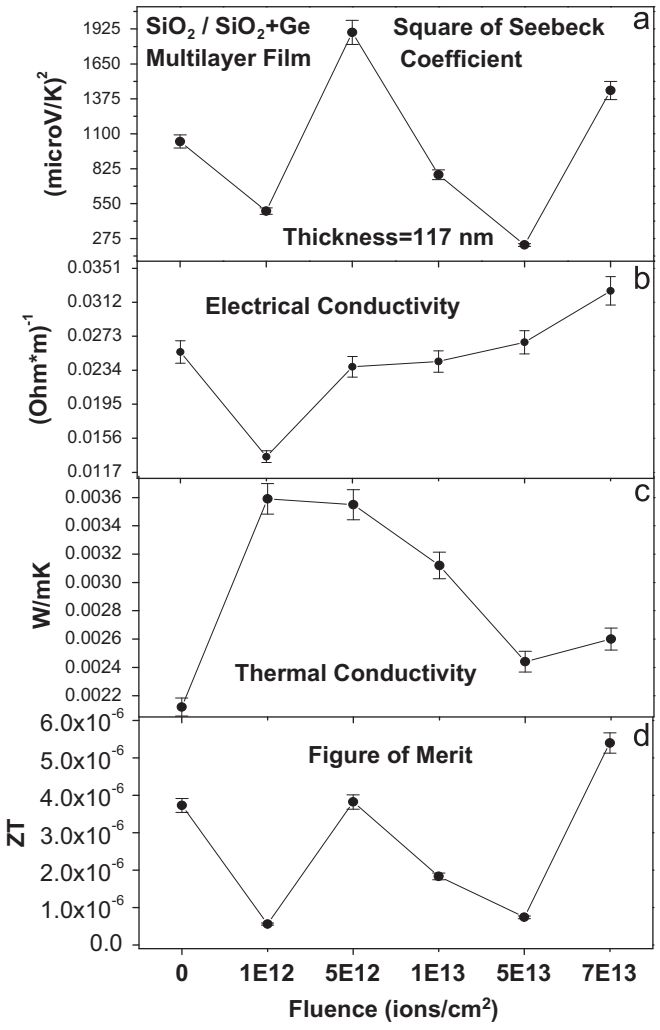

Fig. 4. Thermoelectric properties of 50 alternating nanolayers of SiO_2/SiO_2+Ge multi-layer thin films.

single crystal of the Si substrate at 610 cm^{-1}. Then, a broad peak is present close to another Si band at 1000 cm^{-1}. This band is not as defined as the one at 610 cm^{-1}. At also, like the amorphous layers the intensity of the peak in these regions decrease as a function of ion fluence.

Fig. 4 shows the thermoelectric properties of 50 alternating layers of SiO_2/SiO_2+Ge virgin (unbombarded) and 5 MeV Si ions bombarded thin films at five different fluences. Fig. 4a shows the square of the Seebeck coefficient of the thin film systems. The original Seebeck values are negative that is, we have negative thermo-power and electrons are the main charge carriers. The virgin sample has the Seebeck coefficient of –32.23 μV/K at the room temperature and this value decreased from this value until maximum value of -43.57 μV/K at the fluence of 5×10^{12} ions/cm^2. When the MeV Si ions bombardment was continued at the increasing fluences at the room temperature, the Seebeck coefficient reached -37.96 μV/K at the fluences of 7×10^{13} ions/cm^2. At the other fluences at the room temperature, we could not reach higher Seebeck coefficient than what the virgin sample has of -32.23 μV/K. Enhancement of the Seebeck coefficient without reducing the electrical conductivity is essential to realize practical thermoelectric materials exhibiting a dimensionless figure of merit exceeding 2. Hiromichi Ohta et al. demonstrated that a high-density two dimensional electron gas confined within a unit cell layer thickness in $SrTiO_3$ yields unusually large, approximately five times larger than that of $SrTiO_3$ bulks, while maintaining a high electrical conductivity (Ohta et al., 2007). A.S. Alexandrov and A. M. Bratkovsky studied giant thermopower and figure of merit of semiconducting polaronic nanolayers (Alexandrov and Bratkovsky 2010). In this study, they have showed that polarons – electrons coupled with lattice vibrations – play a key role in transport and optical properties of many semiconductors. They calculated the energy spectrum and thermopower of Fröhlich polarons confined to a potential well as a function of the well thickness. As a result they have reached the fact that the polaron mass enhancement in $2+\epsilon$ dimensions explains a giant thermoelectric power recently observed in doped semiconducting nanolayers (multiple quantum wells) and proposed a route for enhancing the performance of thermoelectric energy nano-converters by increasing their figure of merit by more than one order of magnitude. The observed effects of Si ion bombardment have the opposite characteristics for the electrical and the thermal conductivity values as function of varying fluence, as shown in the Figs. 4b and c respectively while the ion beam fluences are being increased. As seen from Fig. 4b, the remarkable increase in the electrical conductivity was observed at the fluence of 7×10^{13} ions/cm^2.

Electrons (or holes) and phonons have two length scales associated with their transport, wavelength and mean free path. By nanostructuring semiconductors with sizes comparable to the wavelength, sharp edges and peaks in their electronic density of states are produced, whose location in energy space depends on size. By matching the peak locations and shape with respect to the Fermi energy, one could tailor the Seebeck coefficient. Furthermore, such quantum confinement also increases electronic mobility, which could lead to high values of the electrical conductivity. Hence, quantum confinement allows manipulation of the Seebeck coefficient square time the electrical conductivity (Majumdar 2004). Even the study in Ref. Ohta et al., (2007) showed more increase in the figure of the merit of the nanosturctures with respect to the bulk materials, the sharp edges and peaks in the density of states due to confinement are not sufficient to explain the figure of merit measured in Ref. Majumdar (2004). However, the study in Ref. Alexandrov and Bratkovsky (2010) could help us to improve our multi-nanolayered thin film systems using their explanations and methods used for the multiple quantum wells like our multi-nanolayered thin films and might enable us to work together with this group for better thermoelectric devices. As seen from Fig. 4c, the thermal conductivity value increased when the first ion bombardment was introduced at the fluence of 1×10^{12} ions/cm^2 and then the thermal conductivity started to decrease after the fluence 1×10^{12} ions/cm^2 and continued until the fluence of 5×10^{13} ions/cm^2. The turning points for the thermal conductivity are the fluence of 1×10^{12} ions/cm^2 and 5×10^{13} ions/cm^2. Theodorian Borca-Tasiuc

et al. used the 3ω technique to measure the cross-plane thermal conductivity of the symmetrically strained Si/Ge superlattices. Their experimental results indicated a strong reduction in the thermal conductivity of the symmetrically strained Si/Ge superlattices relative to the Si/Ge alloy film. Their thermal conductivity values varied from 2.9 to 4.0 $Wm^{-1}K^{-1}$ at room temperature (Borca-Tasiuc et al., 2000). In our superlattice system, we have prepared the SiO_2/SiO_2+Ge amorphous multilayer films. Since the high energy Si ion bombardments form nanodots and/or nanoclusters in the multilayer thin films, these formations cause phonon scattering and quantum confinement in the multilayer thin film systems to cause a reduction in the cross-plane thermal conductivity. Our cross plane thermal conductivity values take the values between 0.0022 and 0.0036 $Wm^{-1}K^{-1}$ at room temperature at the different applied ion beam fluences. Alexander Balandin and Kang L. Wang studied the effects of phonon spatial confinement and showed that the thermoelectric figure of merit is strongly enhanced in quantum wells and superlattices due to spatial confinement of acoustic phonons. They have shown that strong modification of the phonon group velocities and dispersion due to spatial confinement leaded to a significant increase of the phonon relaxation rates and as a result, a strong drop in the thermal conductivity. From the numerical calculations, they found that due to decrease of the thermal conductivity, the thermoelectric figure of merit experienced an additional increase as compared to the structures with bulk phonons (Balandin and Wang 1998). Fig. 4d shows the calculated dimensionless figure of merit, ZT values by applying the equation given in the introduction part. The desired results of ion bombardment on ZT strongly appear at the fluences of 5×10^{12} ions/cm^2 and 7×10^{13} ions/cm^2.

4. Conclusion

We have deposited the 50 alternating layers of SiO_2/SiO_2+Ge nanolayers thin films on silicon and silica (suprasil) substrates with the ion beam assisted deposition (IBAD). By using the Raman Spectra and its analysis we reached the information about the order and bond structures of the elements in the multilayered systems. The thermoelectric properties have been characterized under the effect of MeV Si ions bombardments at the five different fluences. The first desired identity for the efficient thermoelectric device and materials is the high electrical conductivity and high Seebeck coefficient. The second one is the low thermal conductivity. As seen from the Fig. 4, we have reached the higher Seebeck coefficient and the electrical conductivity, and the low thermal conductivity at the suitable fluences. Since the thermoelectric devices could be used in many applications at the different ranges of temperatures, we will be working on SiO_2/SiO_2+Ge thin film systems at the different temperature ranges to reach higher efficiency for the different purposes.

Acknowledgment

Research sponsored by the Center for Irradiation of Materials (CIM), National Science Foundation under NSF-EPSCOR R-II-3 Grant No. EPS-1158862, NSF-MRSEC Grant# DMR0820382, DOD under Nanotechnology Infrastructure Development for Education and Research through the Army Research Office # W911 NF-08-1-0425.

References

Alexandrov, A.S., Bratkovsky, A.M., 2010. Phys. Rev. B 81, 152204.
Balandin, Alexander, Wang, Kang L., 1998. Journal of Applied Physics 84, 6149.
Borca-Tasiuc, Theodorian, Liu, Weili, Liu, Jianlin, Zeng, Taofang, Song, David W., Moore, Caroline D., Chen, Gang, Wang, Kang L., Goorky, Mark S., Radetic, Tamara, Gronsky, Ronald, Koga, Takaaki, Dresselhaus, Mildred S., 2000. Superlattices and Microstructures 28, 199.
Bourgault, D., Giroud Garampon, C., Caillault, N., Carbone, L., Aymami, J.A., 2008. Thin Solid Films 516, 8579–8583.
Brian, C., 2002. Scales, Science 295, 1248.
Budak, S., Muntele, C., Zheng, B., Ila, D., 2007. Nuc. Instr. and Meth. B 261, 1167.
Budak, S., Guner, S., Muntele, C., Ila, D., 2009. Nuc. Instr. and Meth. B 267, 1592–1595.
Cahill, D.G., Katiyar, M., Abelson, J.R., 1994. Phys. Rev.B 50, 6077.
Dughaish, Z.H., 2002. Physica B 322, 205.
Goldsmid, H., 1964. Thermoelectric Refrigeration. Plenum Press, New York.
Gole, J.L., Dixon, D.A., 1998. J. Phys. Chem. B 102, 33.
Guner, S., Budak, S., Minamisawa, R.A., Muntele, C., Ila, D., 2008. Nuc. Instr. and Meth. B 266, 1261.
Holland, L.R., Smith, R.C., 1966. J. Apl. Phys 37, 4528.
Huang, B.C.-K., Lim, J.R., Herman, J., Ryan, M.A., Fleural, J.-P., Myung, N.V., 2005. Electrochemical Acta 50, 4371.
Huesgen, Till, Woias, Peter, Kockman, Norbert, 2008. Sensors and Actuators A 145–146, 423–429.
Klein, P.B., Masui, H., Song, J., Chang, R.K., 1974. Solid State Commun. 14, 1163.
Majumdar, Arun, 2004. Science 303, 777.
Ohta, Hiromichi, Kim, Sungwing, Mune, Yoriko, Mizoguchi, Teruyasu, Nomura, Kenji, Ohta, Shing, Nomura, Takashi, Nakashi, Yuki, Ikuhara, Yuichi, Hirano, Masahiro, Hosno, Hideo, Koumoto, Kunithito, 2007. Nature Materials 6, 129.
Riffat, S.B., Ma, Xiaoli, 2003. Applied Thermal Engineering 23, 913–935.
Slack, G., 1995. In: Rowe, D.M. (Ed.), CRC Handbook of Thermoelectrics. CRC Press, pp. 407.
Tasciuc, T.B., Kumar, A.R., Chen, G., 2001. Rev. Sci. Instrum 72, 2139.
Xi, Hongxia, Luo, Lingai, Fraisse, Gilles, 2007. Renewable and Sustainable Energy Reviews 11, 923–936.
Xiao, Feng, Hangarter, Carlos, Yoo, Bongyoung, Rheem, Youngwoo, Lee, Kyu-Hwan, Myung, Nosang V., 2008. Electrochimica Acta 53, 8103–8117.
Xiao, Feng, Hangarter, Carlos, Yoo, Bongyoung, Rheem, Younwoo, Lee, Kyu-Hwan, Myung, Nosang V., 2008. Electrochimica Acta 53, 8103–8117.